RAPID COMMUNICATIONS

PHYSICAL REVIEW E VOLUME 49, NUMBER 3 MARCH 1994

Density waves of granular flow in a pipe using lattice-gas automata

Gongwen Peng* and Hans J. Herrmann
Höchstleistungsrechenzentrum, Forschungszentrum Jülich, D-52425 Jülich, Germany
(Received 8 November 1993)

We use a lattice-gas automaton modeling the formation of density waves of granular flow through a vertical pipe. It is found that both the dissipation and the roughness of the walls of the pipe are essential to the emergence of density waves. The density waves can only be observed when the average density of the system is in a certain range. The power spectra of density fluctuations in one region in the pipe follow, apart from a sharp peak corresponding to the density wave, a power-law spectrum $1/f^{\alpha}$ with α close to $\frac{4}{3}$.

PACS number(s): 05.20.Dd, 47.50.+d, 47.20.−k, 46.10.+z

Granular materials exhibit many unusual phenomena, such as size segregation [1–4], heap formation and convection cells under vibration [5–8], and anomalous sound propagation [9,10]. Even in simple geometries such as hoppers and pipes, their flow under gravity still shows complex dynamics [11,12]. Experiments [11,12] and molecular-dynamics (MD) simulations [12–14] show that the granular particles do not flow uniformly but rather form density waves (or shock waves) where regions of high density travel with velocity different from that of the average velocity. In the experiment of flow in a hopper Baxter *et al.* [11] found that density waves only existed when rough sands were used. To understand the density waves in granular flow, attempts have been made by computer simulations with MD [12–14] and the kinetic wave approach [14,15]. The mechanism for the density waves is, however, not really clarified so far.

The present work is to study this problem from another point of view, namely the lattice-gas automaton (LGA) which was first introduced as a novel alternative to traditional methods for numerically solving the Navier-Stokes equation [16]. As a sort of primitive molecular-dynamics system it offers the advantage of guaranteed numerical stability coupled with extreme computational simplicity. We are interested in the density waves in a vertical narrow pipe which were observed experimentally by Pöschel [12] and simulated with MD by him and later by Lee [14]. We consider a LGA at integer times steps $t=0,1,2,\ldots$ with N particles located at the sites of a two-dimensional (2D) triangular lattice which is L sites long vertically and W sites wide horizontally. Periodic boundary conditions are used in the vertical direction while fixed boundary conditions are set for the walls. At each site there are seven Boolean states which refer to the velocities, $\mathbf{v}_i (i=0,1,2,\ldots,6)$. Here $\mathbf{v}_i$ $(i=1,2,\ldots,6)$ are the nearest-neighboring (NN) lattice vectors and $\mathbf{v}_0=0$ refers to the rest (unmoving) state. Each state can be either empty or occupied by a single particle. Therefore the number of particles per site has a maximal value of 7 and a minimal value of 0. The time evolution of LGA consists of a collision step and a propagation step. In the collision step particles change their velocities due to collisions and in the subsequent propagation step particles move in the directions of their velocities to the NN sites where they collide again.

The system is updated in parallel. Only the following specified collisions can deviate the trajectories of particles. All collisions conserve mass and momentum.

Let us number the six bonds connected to a site counterclockwise, with an index i, defined as the integers (mod6), $i=1,2,\ldots,6$, and label the rest particle with index 0. We consider only two- and three-body collisions.

For two-body collisions, we have the following.

(1) $(i,i+3)$ goes to $(i+1,i-2)$ and $(i-1,i+2)$ with equal probability of $\frac{1}{2}$. Here $(i,i+3)$ means two particles with opposite velocities making a head-on collision (this notation was also used in [16]).

(2) $(i,i+2)$ goes to $(0,i-2)$ with probability of p and $(i+3,i-1)$ with probability of $1-p$. If p is nonzero, this means that the energy is dissipated due to collision. This is the case for rough granular particles.

For three-body collision, we have the following.

(3) $(i,i+2,i-2)$ goes to $(0,i,i+3),(0,i-1,i+2)$, $(0,i+1,i-2)$ with probability of $p/3$ for each, and $(i+3,i+1,i-1)$ with probability of $1-p$.

The collision rules for moving particles with a rest particle involve typical mechanisms of granular flow [17,18]. Intuitively one can understand them as follows. Rest particles in a region will decrease the local granular temperature which can be regarded to be the (kinetic) energy, causing a decrease in pressure in that region. The resulting pressure gradient will lead to a migration of particles into that region, increasing its density and decreasing its pressure and granular temperature even more. That means that rest particles will induce having more rest particles nearby. However, due to the restriction of the LGA that the rest state at one site can at most be occupied by one particle, we cannot simulate the above-mentioned mechanisms easily. For example, two moving particles colliding with a rest particle from opposite directions can stop each other in accordance with momentum conservation. But on each site only one rest particle is allowed. Therefore the collision should be tak-

*Permanent address: Institute of Physics, Academia Sinica, Beijing, China.

en by an off-site collision, i.e., the two particles stay at rest on the NN sites where they originally came from. However, on these sites there may already exist other rest particles. To make things easy, we will still use the on-site collision but temporarily allow more than one particle on a site during the collision. Immediately after the collision, the extra rest particles hop to NN sites randomly until they find a suitable site with no rest particle already sitting there. Only in this way can we incorporate the mechanisms mentioned above. The collision rules with rest particles are as follows.

(4) $(i,0,i+3)$ goes to (0,0,0) with certainty.

(5) $(i,0,i+2)$ goes to $(0,0,i-2)$ with certainty.

So far, we have not considered the gravity which is the driving force of the flow. We simply incorporate it by the following rule.

(6) A rest particle decides to have a velocity along the direction of gravity with probability g, if the resulting state is empty at that time. A moving particle colliding with a rest particle can change its velocity by a unit vector along gravity with probability g, if the resulting state is possible on the triangular lattice used.

The sites at the walls of the system only have two directions into which the particles can move. So, the collision rule with the walls reads as follows.

(7) A particle colliding with the wall from one direction can be bounced back with probability b and specularly reflected into the other direction with probability $1-b$. If $b=0$, the walls are smooth (perfect no-slip condition). Otherwise, the walls have some roughness.

We evolve the system according to the collision rules defined above. The initial configuration of the system is set to be random in the sense that each state (except the rest state) of each site is randomly occupied according to a preassigned average density ρ. In the following we report the results made on systems with length $L=2200$ and width $W=11$. The lattice spacing is taken to be the unit and the triangular lattice has an axis parallel to gravity and to the walls.

Figure 1(a) shows the time evolution of the density in the pipe measured every 80 time steps from $t=1$ to $t=40\,000$ for $p=0.1$, $g=0.5$, $b=0.5$. The average density of the system is $\rho=1.0$ (note that the range of ρ is between 0 and 7). The density plots are made as follows. We divide the pipe along the vertical direction into 220 bins with equal length of 10 (total length $L=2200$) and count the number of particles n_i in the ith bin. The gray scale of each bin is a linear function of n_i. The $n_i(i=1,2,\ldots)$ at a given time are plotted from top to bottom while densities at different time steps are plotted from right to left as time increases. Gravity is from top to bottom. We see that initially the density is rather uniform and gradually regions of high density are being formed out of the homogeneous system. A high-density region may also die out and two high-density regions may merge to form a single one. It seems clear that these are the same density waves (or shock waves) which were also observed in experiments [11,12] and MD simulations [12–14]. We also found that the width of the density wave initially increases with time and then saturates after many time steps. For most of the time, these density waves just travel with almost constant velocity which depends on the parameters (p,g,b,ρ) used. This constant velocity was also noted in MD simulations [14]. We have

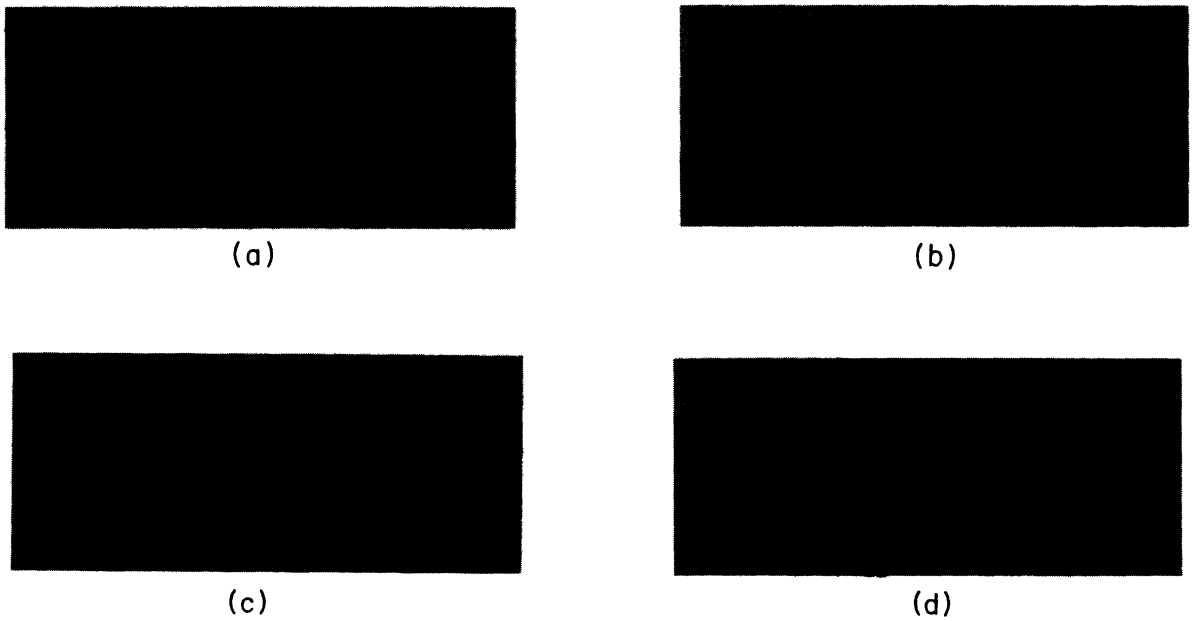

FIG. 1. Time evolution of the density n_i $\{i=1,2,\ldots,220\}$ in the 220 bins in the pipe of $L=2200$, $W=11$, and $\rho=1.0$. Densities at a given time are plotted from top to bottom (direction of gravity) while densities at different time steps are plotted from right to left (direction of time increase) every 80 time steps during 40 000 time steps. The gray scale of each bin is a linear function of n_i. Darker regions correspond to higher densities. (a) $p=0.1$, $g=0.5$, $b=0.5$; (b) $p=0$, $g=0.5$, $b=0.5$; (c) continued from (b) but with dissipation switched on by setting $p=0.1$; (d) $p=0.1$, $g=0.5$, $b=0$.

checked that the density waves do not disappear for very long time steps. For systems with length $L=220$, we still found density waves after 2×10^6 time steps. It seems to us that the density waves are permanently present.

The average density ρ plays an important role in the formation of density waves. We found that the density waves can only be observed in a certain range of ρ. This range is almost independent of p, g, and b and is approximately between 0.6 and 1.6. This range might be understood as follows. For very low density, the interactions among the particles are so few that no collective phenomena can be observed. For high density, the system would more or less behave as a solid and lose some fluid properties due to space-filling constraints. Therefore, high density is not suitable for the density wave formation either. Only within a range can the density wave be observed.

The difference between the "granular gas" and a regular gas is in the inherent dissipative nature of the elementary collision processes. Here we include the dissipation through the parameter p. If we switch off p, no dissipation is present. In such a case, strikingly, the density waves do not form. This is shown in Fig. 1(b), which is otherwise the same as Fig. 1(a) except for $p=0$. From this we can conclude that the dissipation among the particles is essential to the formation of density waves (this was experimentally observed by Baxter *et al.* in a hopper [11]).

One advantage of simulations is that one can easily control and modify the dynamical process. From $t=1$ to $t=40\,000$ we switch off the dissipation, and the results are in Fig. 1(b). Now starting from $t=40\,000$, we switch the dissipation on by setting $p=0.1$, and we obtain the results of Fig. 1(c) where density waves are observed again. This reveals that even for a minute degree of dissipation (provided p is nonzero), its mere existence gives rise to significantly different physics as compared to that of regular gases and liquids.

The roughness of walls is also essential to the density wave formation. When we turn off the roughness parameter b ($b=0$), we observe no density waves either. This is shown in Fig. 1(d).

To characterize the density fluctuations in a certain region with time, we calculate their power spectra. We did this in a system of length $L=220$ and width $W=11$. We recorded the number of particles in a vertical region of length 10 every 10 time steps. The dynamical process is performed for very long time steps so that we obtain $256K$ ($1K=1024$) data to analyze for each power spectrum. We first subtract the mean value from the data, otherwise there would be a huge peak at $f=0$ in the power spectra. We calculated the spectra using a standard fast Fourier transform (FFT) routine. To get better statistics, an average process has been used. We broke the time series of $256K$ points into S segments of M points each. On each segment an FFT was performed using a Parzen window [19] and the powers of the resulting spectra were averaged. Here we used $S=4$. A representative power spectrum is shown in Fig. 2 for $p=0.5$, $g=0.5$, $b=0.5$, $\rho=1.0$. The frequency is in an arbitrary unit and can be related to the real time period (we check this relation by using the same program to analyze a series of exactly periodic data with the same number of points). The frequency $f=1000$ in Fig. 2 corresponds to a time period of $T=328$. In Fig. 2 we observe that a sharp peak exists around $f=596$. The time period of this peak is $T=328\,000/596=550$ and corresponds to a wave velocity of $v=L/T=\frac{220}{550}=0.4$. This value coincides very well with the velocity we measured for the density waves directly from the time-evolution plots of density [similar to Fig. 1(a) but for $p=0.5$]. That is to say, the highest-density region traveling periodically in the system [see Fig. 1(a)] contributes to the power spectrum a sharp peak. From Fig. 2 one sees that apart from this peak there is a power-law regime where the spectrum falls off as $1/f^{\alpha}$. The line in the log-log plot of Fig. 2 represents a least-squares fit to the points between $f=40$ and 1000 after subtracting the sharp peak. The exponent is $\alpha=1.33\pm0.02$ ($\simeq\frac{4}{3}$). Our ability to study the behavior in the very low frequency regime ($f<40$) was limited by the long time series of data required. The exponent α is found to be independent of the parameters used but the position of the sharp peak (therefore the velocity of the density wave) does depend on the parameters.

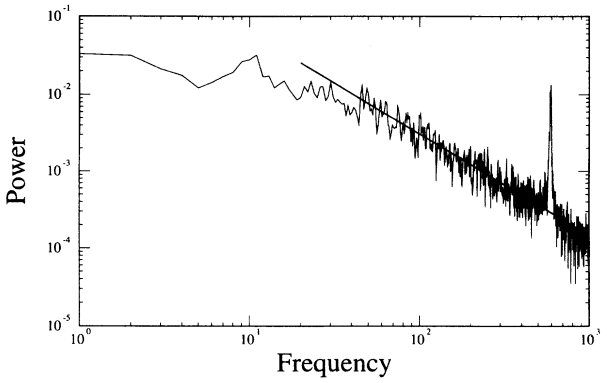

FIG. 2. Power spectrum of the time series of the density fluctuation inside a certain region in a pipe of $L=220$ and $W=11$. Parameters used here are $p=g=b=0.5$, $\rho=1.0$. The straight line is least-squares fit with a slope of -1.33 ± 0.02.

The picture revealed by Fig. 2 is rather clear. In Fig. 1(a) we observed the high-density region traveling periodically due to the periodic boundary condition. This wave is very strong and most clearly distinguished from the rest. This is why the peak in Fig. 2 is so high. Apart from this wave, there are also other waves with a broad range of frequencies (or traveling velocities). The spectrum of these waves follows a power-law distribution $1/f^{\alpha}$ with α close to $\frac{4}{3}$, which might be associated with the dissipation instability discussed in [17,18].

In conclusion, by using a lattice-gas model we observed the density waves found in experiments and MD simulations. The density waves exist only in a range of average densities. Both the dissipation among the granular particles and the roughness of the walls of pipes are essential to the formation of such traveling waves which might be similar to the kinetic waves also observed in traffic jams [20]. The density fluctuations follow, apart from a sharp

peak corresponding to the density wave discussed above, a $1/f^{\alpha}$ power spectra with α close to $\frac{4}{3}$. Power-law spectra have also been observed in experiments [11,12] and MD simulations [13] and we conjecture that they are a direct consequence of the dissipation instability [17,18]. The formation of density waves and the $1/f^{\alpha}$ power spectra is a rather complex phenomenon and further work should be devoted to explain its mechanism.

We acknowledge the members of the Höchstleistungsrechenzentrum Many Body Group for stimulating discussions. Special thanks to Jan Hemmingsson for constant conversation.

[1] J. C. Williams, Powder Technol. **15**, 245 (1976).
[2] P. K. Haff and B. T. Werner, Powder Technol. **48**, 239 (1986).
[3] A. Rosato, K. J. Strandburg, F. Prinz, and R. H. Swendsen, Phys. Rev. Lett. **49**, 59 (1987).
[4] P. Devillard, J. Phys (Paris) **51**, 369 (1990).
[5] M. Faraday, Philos. Trans. R. Soc. London **52**, 299 (1831).
[6] P. Evesque and J. Rajchenbach, Phys. Rev. Lett. **62**, 44 (1989).
[7] Y. H. Taguchi, Phys. Rev. Lett. **69**, 1367 (1992).
[8] J. A. C. Gallas, H. J. Herrmann, and S. Sokolowski, Phys. Rev. Lett. **69**, 1371 (1992).
[9] C-h. Liu and S. R. Nagel, Phys. Rev. Lett. **68**, 2301 (1992).
[10] H. M. Jaeger and S. R. Nagel, Science **255**, 1523 (1992).
[11] G. W. Baxter, R. P. Behringer, T. Fagert, and G. A. Johnson, Phys. Rev. Lett. **62**, 2825 (1989).
[12] T. Pöschel, HLRZ Report No. 67/92, 1992 (unpublished).
[13] G. Ristow and H J. Herrmann, HLRZ Report No. 7/93, 1993 (unpublished).
[14] J. Lee, HLRZ Report No. 44/93, 1993 (unpublished).
[15] M. Leibig, HLRZ Report No. 42/93, 1993 (unpublished); J. Lee and M. Leibig, HLRZ Report No. 49/93, 1993 (unpublished).
[16] U. Frisch, B. Hasslacher, and Y. Pomeau, Phys. Rev. Lett. **56**, 1505 (1986).
[17] S. Savage, J. Fluid Mech. **241**, 109 (1992).
[18] I. Goldhirsch and G. Zanetti, Phys. Rev. Lett. **70**, 1619 (1993).
[19] W. H. Press, B. P. Flannery, S. A. Teukolsky, and W. T. Vetterling, *Numerical Recipes in C* (Cambridge University Press, Cambridge, England, 1988).
[20] K. Nagel and M. Schreckenberg, J. Phys. (France) I **2**, 2221 (1992).

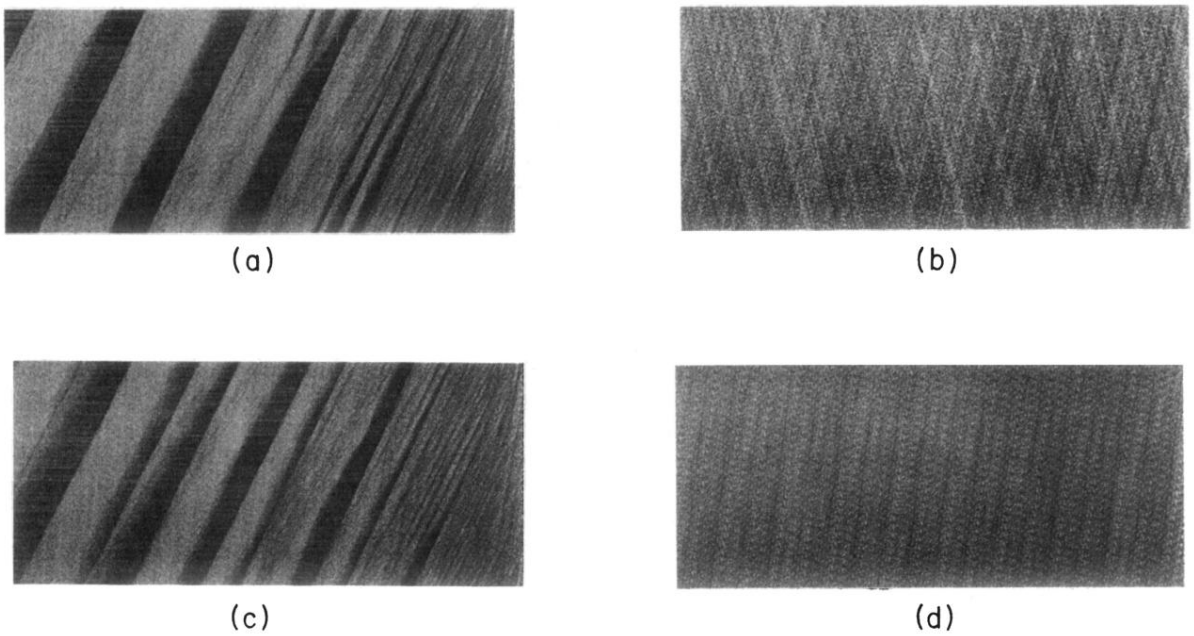

FIG. 1. Time evolution of the density n_i $\{i=1,2,\ldots,220\}$ in the 220 bins in the pipe of $L=2200$, $W=11$, and $\rho=1.0$. Densities at a given time are plotted from top to bottom (direction of gravity) while densities at different time steps are plotted from right to left (direction of time increase) every 80 time steps during 40 000 time steps. The gray scale of each bin is a linear function of n_i. Darker regions correspond to higher densities. (a) $p=0.1$, $g=0.5$, $b=0.5$; (b) $p=0$, $g=0.5$, $b=0.5$; (c) continued from (b) but with dissipation switched on by setting $p=0.1$; (d) $p=0.1$, $g=0.5$, $b=0$.